Impact of Heat Treatment and Composition of ZnO–TiO2 Nanoparticles for Photocatalytic Oxidation of an Azo Dye

ARTICLE *in* INDUSTRIAL & ENGINEERING CHEMISTRY RESEARCH · FEBRUARY 2008

Impact Factor: 2.59 · DOI: 10.1021/ie071255p

Impact of Heat Treatment and Composition of $ZnO-TiO_2$ Nanoparticles for Photocatalytic Oxidation of an Azo Dye

William L. Kostedt, IV,*,† Adel A. Ismail,‡ and David W. Mazyck†

Department of Environmental Engineering Sciences, University of Florida, 321 A.P. Black Hall, P.O. Box 116450, Gainesville, Florida 32611-6450, and Central Metallurgical Research and Development Institute (CMRDI), P.O. Box 87, Helwan 11421, Cairo, Egypt

TiO_2-ZnO mixed oxide nanoparticles were synthesized by precipitation of zinc nitrate and titanium tetrachloride as precursors and then heat treated using two techniques: hydrothermal and calcination. The particles were characterized using XRD, BET, UV diffuse reflectance, and ζ potential techniques. Additionally, the particles were tested for their ability to induce the photocatalytic oxidation and adsorption of Procion Red MX-5B dye. The highest photocatalytic oxidation was observed for nanoparticulate mixed oxides that were near 100% ZnO or TiO_2. These materials did not have the highest specific surface areas, yet it is believed that their near-neutral ζ potentials and ideal band gap energies contributed to their higher photocatalytic activities. XRD patterns indicated that sintering and increased crystallinity occurred for the calcined TiO_2 samples.

1. Introduction

Textile dyes represent a significant environmental hazard to aquatic biota and humans due to their toxicity[1] and tendency to cause eutrophication.[2] Improvements in chemical structure have led to increased longevity of dyed fabrics, yet make the textile wastewater more difficult to treat. Traditional biological methods often fail due to the increased stability of highly aromatic dye molecules. Additionally, methods such as adsorption, reverse osmosis, and coagulation simply transfer the dye from one phase to another, leaving a secondary waste problem.

Photocatalytic oxidation represents an attractive solution due to the ability to completely oxidize organic contaminants to carbon dioxide, water, and mineral acids, hence avoiding the secondary waste problem, yet there are several challenges associated with such an approach. First, the most active photocatalyst materials are typically nanometer particles (<100 nm diameter); hence, they require special techniques to use them in a commercially viable photoreactor. Several proposed methods for accomplishing this include immobilization on a high surface area substrate[3] or confinement and agitation of photocatalyst coated magnetic particles using a magnetic field.[4] In addition, a commercially successful reactor has been designed to separate a slurry of titanium dioxide using a ceramic membrane, which could also be used for other composite photocatalyst materials.[5]

Several options for advanced oxidation exist including wide-band-gap semiconductors. These materials have the ability to generate hydroxyl radicals when exposed to sub-band-gap energy photons (typically in the ultraviolet range). Frequently used wide-band-gap semiconductors include TiO_2,[6−8] ZnO,[6,9,10] CdS,[11] and others; however, TiO_2 is the most popular due to its relatively low toxicity, low cost, and resistance to photocorrosion.[12] The other materials function as photocatalysts, but exhibit photocorrosion in the presence of UV light that drives the photooxidative reactions. This is particularly troublesome for compounds such as CdS, as photocorrosion leads to pollution with a heavy metal;[11] however, several studies have reported superior performance by using ZnO instead of TiO_2.[13,14]

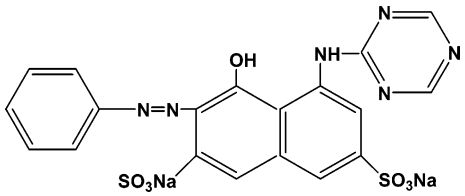

Figure 1. Procion Red MX-5B chemical structure.

While the most frequently used photocatalyst materials are composed of a single semiconductor, other authors have found benefits in using mixed oxides with TiO_2 and one of the following: ZnO, WO_3, SiO_2, or ZrO_2.[15−22] Some explanations for this phenomenon include increased surface acidity and favorable electronic interactions between the different metal oxide materials. In this study, we present the comparison between two heat treatment methods, hydrothermal and calcination, after coprecipitation of ZnO/TiO_2 and explore the role of surface area, heat treatment, zeta (ζ) potential, and band gap energy on photocatalytic oxidation and adsorption of Procion Red MX-5B, an azo dye.

2. Experimental Section

2.1. Materials. All chemicals used in this study were analytical grade reagents. Zinc nitrate hexahydrate $Zn(NO_3)_2 \cdot 6H_2O$ and titanium tetrachloride $TiCl_4$ (Fisher) were chosen as precursors of ZnO and TiO_2, respectively. Procion Red MX-5B was used for photocatalytic oxidation and adsorption experiments.

2.2. Synthesis. $Zn(NO_3)_2 \cdot 6H_2O$ and $TiCl_4$ solutions were mixed at room temperature using magnetic stirring. The samples were synthesized at different compositions, which will be referred to by the percentage of TiO_2 with the balance ZnO followed by "C" for calcined or "H" for hydrothermal (95H corresponds to 95% TiO_2 that was hydrothermally prepared). The pH was adjusted to 8.5 by slowly adding an ammonium hydroxide solution and continuing to stir for 2 h. White $Zn(OH)_2/Ti(OH)_4$ precipitate formed instantaneously. The precipitated samples were divided into two portions to study the effect of direct calcination and hydrothermal techniques. One portion

* To whom correspondence should be addressed. Tel.: (352) 294-0083. Fax: (352) 392-3076. E-mail: kostedt@ufl.edu.
† University of Florida.
‡ CMRDI.

10.1021/ie071255p CCC: $40.75
Published on Web 02/05/2008

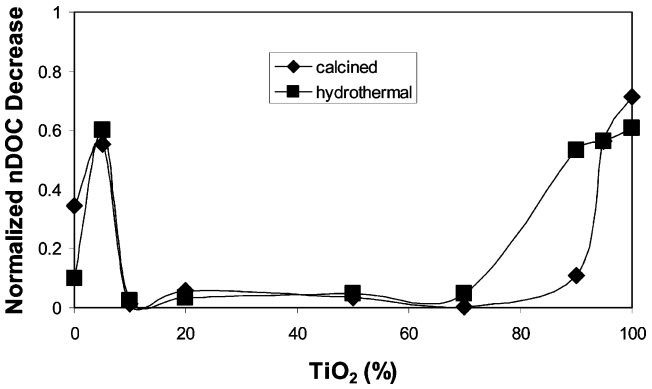

Figure 2. Comparison of photocatalytic oxidation for calcined and hydrothermally prepared ZnO−TiO_2 photocatalyst of varying composition (normalized concentration decrease = $(C_0 - C)/C_0$).

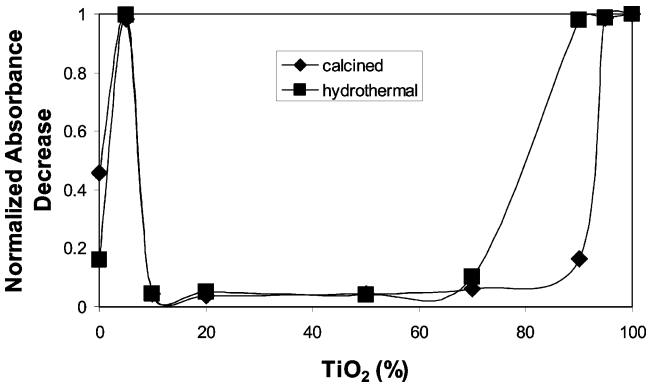

Figure 3. Comparison of color changes for calcined and hydrothermally prepared ZnO−TiO_2 photocatalyst of varying composition (normalized concentration decrease = $(C_0 - C)/C_0$).

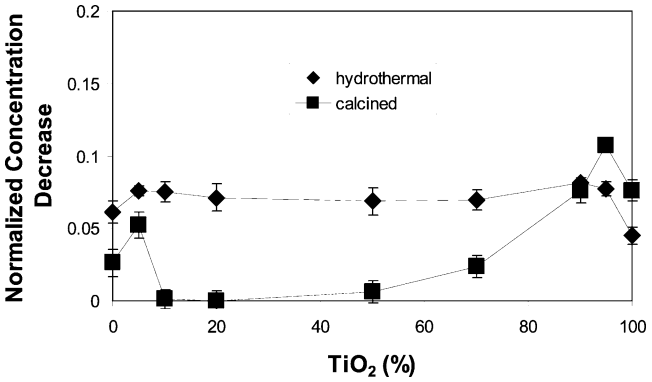

Figure 4. Comparison of Procion Red MX-5B adsorption on ZnO−TiO_2 photocatalyst prepared by calcination and hydrothermal heat treatment (normalized concentration decrease = $(C_0 - C)/C_0$).

was separated by filtration and washed by water several times until the pH reached 7. The first part was dried overnight at 110 °C and calcined at 500 °C for 5 h. The second portion was hydrothermally treated in a Teflon-lined autoclave at 150 °C for 10 h. The powder was then filtered, washed, and dried at 110 °C for 24 h.

2.3. Characterization. Material characterization including specific surface area was estimated using nitrogen adsorption isotherms measured on a Quantachrome Nova 2200e and modeled using the Brunauer−Emmett−Teller (BET) model. X-ray diffraction (XRD) 2θ patterns were derived with a Phillips APD 3720, ζ potential was determined using a Brookhaven ZetaPlus, and diffuse reflectance spectra were estimated using a Labsphere PELA-1000 integrating sphere module in a Perkin-Elmer Lambda 800 UV/vis spectrophotometer.

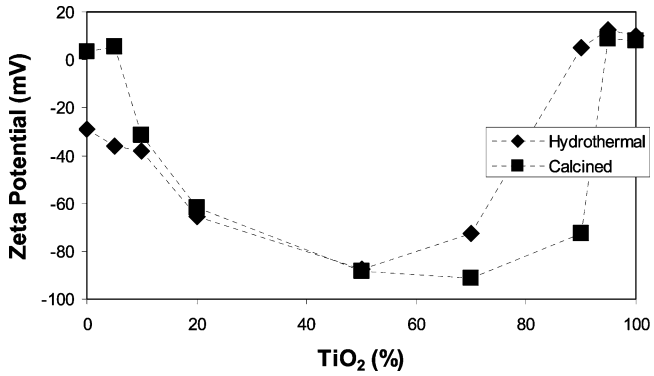

Figure 5. Comparison of ζ potential for a ZnO−TiO_2 photocatalyst prepared by hydrothermal and calcination technique with varying composition.

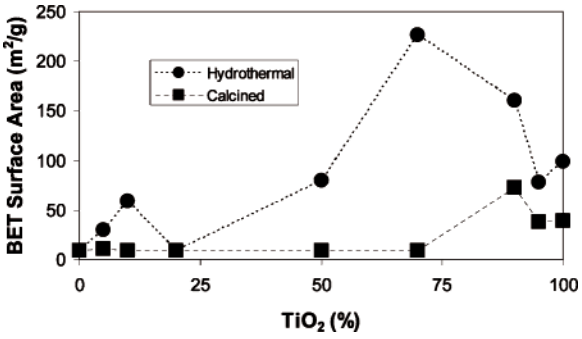

Figure 6. Comparison of BET specific surface area for of ZnO−TiO_2 photocatalyst prepared by hydrothermal and calcination technique with varying composition.

2.4. Dye Photocatalytic Oxidation. Performance of the photocatalyst materials was assessed by measuring both adsorption and photocatalysis of Procion Red MX-5B dye. All experiments were conducted using a Glas-Col Rugged Rotator. Teflon sealed borosilicate vials were prepared with 20 mg of photocatalyst and 40 mL of 15 mg/L Procion Red MX-5B (RR) dye solution (Figure 1), where the pH was unadjusted and measured to be 6.8 ± 0.2. Photolytic degradation of this dye was found to be negligible in previous work by Khan.[23] Dye adsorption was quantified by preparing vials and rotating for 24 h in a dark black box before analysis. Photocatalytic oxidation experiments involved preparing samples in Teflon sealed borosilicate vials in the same manner as in the adsorption experiments, except that an array of four 8 W 365 nm peak output UV bulbs were placed 7.6 cm from the rotator for 3 h. Ferrioxalate actinometry determined the total flux to be 1.01×10^{-5} einsteins/min. RR concentration was measured by first vacuum filtering the samples using a 0.2 μm nitrocellulose membrane filter, and then determining the absorbance of the sample using a Hach DR/4000U spectrophotometer at 538 nm.

3. Results and Discussion

For hydrothermally prepared samples, the trend for the extent of photocatalytic oxidation shows that the highest activity occurs in the samples that are near 100% ZnO or TiO_2 (Figures 2 and 3). Two parameters were chosen to assess the progress of photocatalytic oxidation: dye absorbance and nonpurgeable dissolved organic carbon (nDOC). Absorbance was measured at 538 nm, which is an indication of color. Since oxidative attack of the azo bond is preferential, it is important to also follow the oxidation byproducts with nonpurgeable dissolved organic carbon as these byproducts may be toxic even if the solution appears to be clear. Since it was demonstrated earlier that

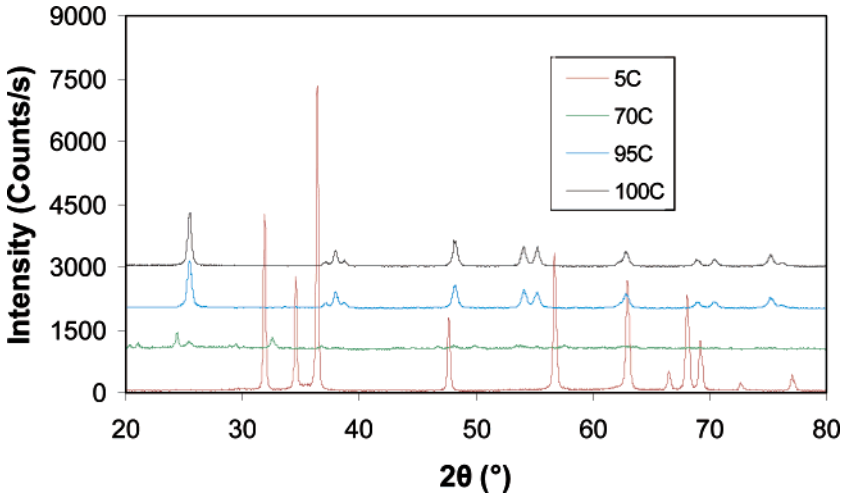

Figure 7. Comparison of XRD patterns of ZnO−TiO_2 photocatalysts prepared using a calcination technique with varying composition.

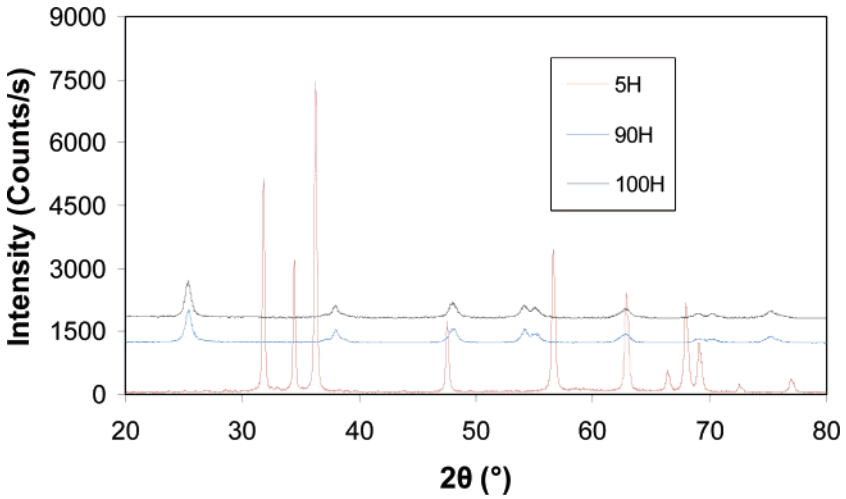

Figure 8. Comparison of XRD patterns of ZnO−TiO_2 photocatalysts prepared using a hydrothermal technique with varying composition.

photolytic oxidation of the dye was negligible, it is thought that the primary mechanism for mineralization is photocatalytic oxidation. Bleaching of the dye as measured by absorbance changes was complete in the 5, 95, and 100% TiO_2 samples of both heat treatments, and the 90% TiO_2 hydrothermal treatment. The highest extent of photocatalytic oxidation (PCO) was for the calcined sample with 100% TiO_2, which still contained 30% of the original organic carbon, presumably as oxidation byproducts. For these samples with 100% absorbance decrease, kinetic information could not be inferred, yet information about the extent of mineralization as determined by nonpurgeable dissolved organic carbon was used for comparison. Additionally, the photocatalytic activity was negligible for samples between 10 and 70% TiO_2.

The relationship between adsorption capacity and photocatalysis is complex, and there is not always a clear correlation between the two phenomena for materials with photocatalytic activity. For instance, previous work with activated carbon demonstrated an increase in adsorption of methylene blue dye on activated carbon that is thought to be due to a change in electron distribution in the dye molecule, which increases adsorption to the aromatic activated carbon basal planes.[23] The photocatalyst prepared using a calcination technique demonstrated a trend of low adsorption and low photocatalytic oxidation between 20 and 90% TiO_2 (Figure 4). It was also interesting to note that the adsorption for the calcined samples roughly followed the ζ potential trend (Figure 5) and was highest at 95% TiO_2, whereas for hydrothermally prepared samples it was relatively constant between 5 and 95%. These trends demonstrate that the higher adsorption capacity of the hydrothermally prepared materials did not translate to higher PCO.

Since RR is an anionic dye and its adsorption and photocatalytic activity have been proven to be related to the pH of solution for TiO_2,[24,25] it was expected that a similar trend might be seen for the mixed oxide materials observed in this work. Electrostatic repulsion by the negatively charged photocatalyst has a tendency to prevent close approach of dye molecules to the reaction sites on the particle surface. Since the PCO reactions occur at or near the surface of the photocatalyst because of the high reactivity of hydroxyl radicals and hence short diffusion distance, it is believed that phenomena which prevent this close approach such as a boundary layer diffusion resistance[4] or electrostatic repulsion[26] have a tendency to reduce PCO. Figure 5 shows the trend for the ζ potential for the various mixed oxide photocalysts. Both photocatalysts demonstrate high negative ζ potentials for compositions between 20 and 70% TiO_2. This region also corresponded to relatively low adsorption and PCO for calcined photocatalysts, as was expected due to electrostatic repulsion. Additionally, the higher performing photocatalysts had near-neutral ζ potential, which corresponds to approximately equal quantities of positively and negatively charged sites on the surface. For calcined samples, the ζ potential was near

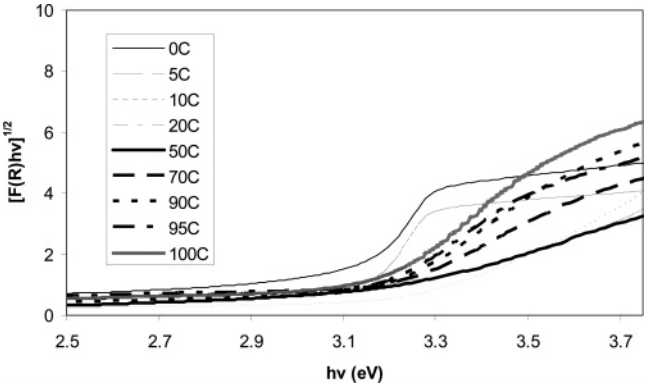

Figure 9. Modified Kubelka−Munk spectra for calcined ZnO−TiO_2 photocatalyst.

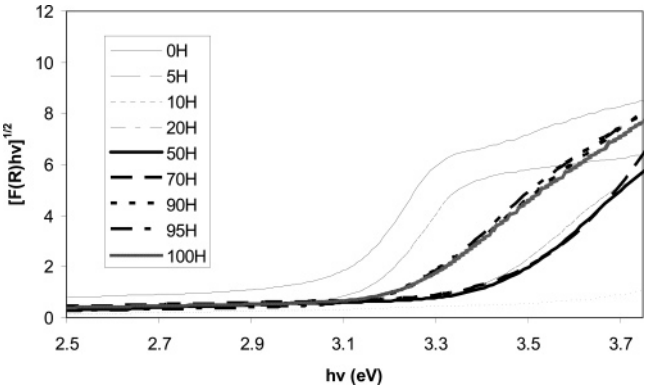

Figure 10. Modified Kubelka−Munk spectra for hydrothermal ZnO−TiO_2 photocatalyst.

neutral for the 0% TiO_2 samples, but was slightly lower for the hydrothermal sample, which may explain the higher PCO for the calcined sample. For the 95 and 100% TiO_2 samples, ζ potential was similar for both preparation methods and approximately neutral, which provided a more ideal environment for PCO.

Specific surface area is often a useful tool for assessing the photocatalytic activity of a material since the reactions likely take place at or near the surface. Higher specific surface areas correspond to more reaction sites available given a constant surface density and quality of reaction sites. This trend is important, but since other variables such as ζ potential, quantum effects, and surface defects can also be a function of particle size for nanometer-sized particles, surface area is not often an ultimate determinant of PCO. From the data that are shown in Figure 6, it is apparent that the highest specific surface area materials are the hydrothermally prepared photocatalyst with 70% TiO_2. Interestingly, this does not correspond to the highest photocatalytic activities or adsorption, which may be due in part to the highly negative ζ potential. Also, those photocatalysts with the highest photocatalytic activity for hydrothermal and calcined samples have specific surface areas of 30.2 and 37.6 m^2/g, respectively, which was in the middle range of all specific surface areas.

X-ray diffraction can provide information about the crystalline structure, composition, and particle size of materials. For photocatalysis, this is important because the crystalline structure and particle size have been proven to have a strong influence on photocatalytic activity.[2] Researchers have demonstrated that calcination of TiO_2 produced using alkoxide precursors can generate anatase or at higher temperatures rutile crystalline phase.[2] The anatase phase has a higher photocatalytic activity,

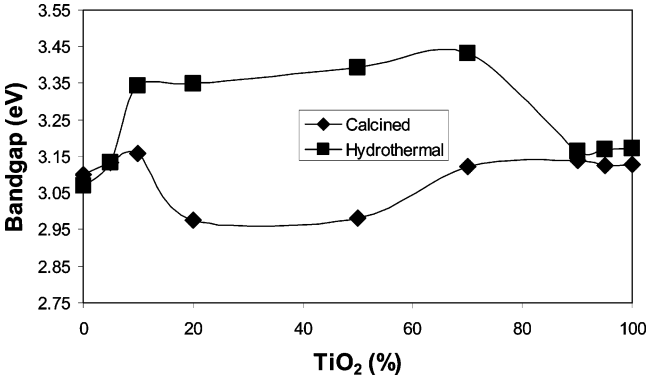

Figure 11. Estimated band gap for calcined and hydrothermally prepared ZnO−TiO_2 photocatalyst materials.

and sintering of TiO_2 produces larger particle size rutile, which has a lower photocatalytic activity than anatase. This is in contrast to Degussa P25, where there is apparently a synergy between the anatase and smaller rutile phase crystals produced by flame synthesis.[27] Figures 7 and 8 show the XRD patterns for several ZnO−TiO_2 samples. The figures show a similar pattern for both 5% TiO_2 samples, with no strong indication of typical anatase or rutile TiO_2 peaks. The pure TiO_2 samples both have anatase (101) plane peaks at about 25.4° 2θ but no rutile (100) plane peaks, indicating that only the anatase crystalline phase is present. Using the Scherrer equation (eq 1), particle size (t) can be estimated based on peak width (B). Given a shape factor (k) of 0.9, λ (wavelength of the Cu $K\alpha_1$ X-ray source) of 0.1541 nm, B (full peak width at half-maximum corrected for instrumental broadening) of 0.0065 and 0.0090 rad for pure TiO_2 calcined and hydrothermally prepared samples, respectively, and 2θ (anatase (101) peak) of 25.4°:

$$t = \frac{k\lambda}{B\cos\theta} \tag{1}$$

The Scherrer equation indicates that particle sizes for the calcined and hydrothermally treated TiO_2 were 21.1 and 16.0 nm, respectively. The larger particle size indicates that sintering has taken place for the calcined TiO_2, which may explain its more intense 101 peak. Either this increase in particle size or an increase in crystallinity is believed to provide a reason for the higher PCO for the calcined photocatalyst. The 5H and 5C samples show characteristic peaks of ZnO at 31.5, 34.3, 36.1, 47.3, 56.0, 62.7, and 67.6 corresponding to (100), (002), (101), (102), (110), (103), and (112) planes, respectively. Even though these samples had 5% TiO_2, they showed no evidence of the characteristic peaks of either anatase or rutile crystalline phases.

Optical properties of photocatalyst materials can have a strong influence on performance. For TiO_2, the relationship between particle size, band gap energy, and performance is well documented.[28] Particle size increases lead to decreases in specific surface area and decrease in band gap energy. For the ZnO−TiO_2 composites explored in this work, band gap energy was estimated with the Kubelka−Munk method using diffuse reflectance spectra. The modified Kubelka−Munk function was determined using eq 2

$$\left(\frac{(1-R)^2}{2R}h\nu\right)^{1/2} \tag{2}$$

where R is the proportion reflected, h is Planck's constant, and ν is the frequency of light. Plots of this parameter were used to determine band gap energy by determining a linear model for

the linear portion of the absorption transition using least-squares regression and extrapolating to zero at the corresponding photon energy.[29] The modified Kubelka−Munk spectra can be seen in Figures 9 and 10, and the corresponding band gap energies can be seen in Figure 11. The increase in band gap energy for the hydrothermally prepared samples between 10 and 70% may be due to an increase in atomic dispersion and decrease in primary particle size as indicated by specific surface area. Additionally, the band gap decrease for the calcined photocatalyst between 20 and 70% TiO_2 is thought to be the result of sintering-related particle size increases and increased interaction between ZnO and TiO_2 induced by calcination.

4. Conclusions

The ZnO−TiO_2 photocatalyst synthesized using two different heat treatment methods provided insight into the characteristics that make a photocatalyst material well-suited for PCO of RR dye. First, it was found that the specific surface area did not correlate directly with PCO. Although hydrothermal heat treatments produced mixed oxide materials with surface areas above 200 m^2/g, this did not appear to improve the photocatalytic activity with respect to the calcined photocatalysts. Instead, it was found that those mixed oxides that were near 100% TiO_2 or ZnO had less negative ζ potential, which is believed to result in less electrostatic repulsion. This reduction in electrostatic repulsion of the negatively charged RR dye molecules provides an explanation for the higher PCO of those samples that were nearly pure TiO_2 or ZnO. Additionally, XRD patterns indicated that the particle size and crystallinity were higher for the calcined than the hydrothermally treated TiO_2. This is believed to help explain the higher photocatalytic activity of the calcined photocatalyst.

Acknowledgment

The authors gratefully acknowledge support from the U.S.−Egypt Science Technology Joint Fund (ENV8-002-005).

Literature Cited

(1) Boschke, E.; Böhmer, U.; Lange, J.; Constapel, M.; Schellenträger, M.; Bley, T. The use of respirometric measurements to determine the toxicity of textile dyes in aqueous solution and after oxidative decolourisation processes. *Chemosphere* **2007**, in press.

(2) Hoffmann, M. R.; Martin, S. T.; Choi, W.; Bahnemann, D. W. Environmental Applications of Semiconductor Photocatalysis. *Chem. Rev.* **1995**, *95* (1), 69−96.

(3) Stokke, J. M.; Mazyck, D. W.; Wu, C. Y.; Sheahan, R. Photocatalytic oxidation of methanol using silica-titania composites in a packed-bed reactor. *Environ. Prog.* **2006**, *25* (4), 312−318.

(4) Kostedt, W. L., IV; Drwiega, J.; Mazyck, D. W.; Lee, S.-W.; Sigmund, W.; Wu, C.-Y.; Chadik, P. Magnetically agitated photocatalytic reactor for photocatalytic oxidation of aqueous phase organic pollutants. *Environ. Sci. Technol.* **2005**, *39* (20), 8052−8056.

(5) Kostedt, W. L., IV; Mazyck, D. W.; Powell, T.; Butters, B. Effect of Photocatalyst Type on Oxidation of Ersatz Water Using a Photocatalytic Reactor with Slurry Separation. In *Proceedings of the 36th International Conference on Environmental Systems, Society of Automotive Engineers (SAE): Norfolk, Virginia, July 17−20, 2006*; 2006-01-2085.

(6) Evgenidou, E.; Fytianos, K.; Poulios, I. Semiconductor-sensitized photodegradation of dichlorvos in water using TiO_2 and ZnO as catalysts. *Appl. Catal., B* **2005**, *59* (1−2), 81−89.

(7) Goncalves, M. S. T.; Oliveira-Campos, A. M. F.; Pinto, E. M. M. S.; Plasencia, P. M. S.; Queiroz, M. J. R. P. Photochemical treatment of solutions of azo dyes containing TiO_2. *Chemosphere* **1999**, *39* (5), 781−786.

(8) Sauer, T.; Neto, G. C.; Jose, H. J.; Moreira, R. F. P. M. Kinetics of photocatalytic degradation of reactive dyes in a TiO_2 slurry reactor. *J. Photochem. Photobiol., A* **2002**, *149* (1−3), 147−154.

(9) Curri, M. L.; Comparelli, R.; Cozzoli, P. D.; Mascolo, G.; Agostiano, A. Colloidal oxide nanoparticles for the photocatalytic degradation of organic dye. *Mater. Sci. Eng., C* **2003**, *23* (6−8), 285−289.

(10) Daneshvar, N.; Salari, D.; Khataee, A. R. Photocatalytic degradation of azo dye acid red 14 in water on ZnO as an alternative catalyst to TiO_2. *J. Photochem. Photobiol., A* **2004**, *162* (2−3), 317−322.

(11) Neppolian, B.; Choi, H. C.; Sakthivel, S.; Arabindoo, B.; Murugesan, V. Solar/UV-induced photocatalytic degradation of three commercial textile dyes. *J. Hazard. Mater.* **2002**, *89* (2−3), 303−317.

(12) Kostedt, W. L., IV; Mazyck, D. W. Evaluation of a Photocatalytic Water Treatment Process. *Fl. Water Resour. J.* **2006**, *58* (11), 44−48.

(13) Peralta-Zamora, P.; Kunz, A.; de Moraes, S. G.; Pelegrini, R.; Moleiro, P. D.; Reyes, J.; Duran, N. Degradation of reactive dyes I: A comparative study of ozonation, enzymatic and photochemical processes. *Chemosphere* **1999**, *38* (4), 835−852.

(14) Sakthivel, S.; Neppolian, B.; Shankar, M. V.; Arabindoo, B.; Palanichamy, M.; Murugesan, V. Solar photocatalytic degradation of azo dye: comparison of photocatalytic efficiency of ZnO and TiO_2. *Sol. Energy Mater. Sol. Cells* **2003**, *77* (1), 65−82.

(15) Liao, S. J.; Huang, D. G.; Yu, D. H.; Su, Y. L.; Yuan, G. Q. Preparation and characterization of ZnO/TiO_2, SO_4^{2-}/ZnO/TiO_2 photocatalyst and their photocatalysis. *J. Photochem. Photobiol., A* **2004**, *168* (1−2), 7−13.

(16) Wu, C. H. Comparison of azo dye degradation efficiency using UV/single semiconductor and UV/coupled semiconductor systems. *Chemosphere* **2004**, *57* (7), 601−608.

(17) Marci, G.; Augugliaro, V.; Lopez-Munoz, M. J.; Martin, C.; Palmisano, L.; Rives, V.; Schiavello, M.; Tilley, R. J. D.; Venezia, A. M. Preparation characterization and photocatalytic activity of polycrystalline ZnO/TiO_2 systems. 1. Surface and bulk characterization. *J. Phys. Chem. B* **2001**, *105* (5), 1026−1032.

(18) Marci, G.; Augugliaro, V.; Lopez-Munoz, M. J.; Martin, C.; Palmisano, L.; Rives, V.; Schiavello, M.; Tilley, R. J. D.; Venezia, A. M. Preparation characterization and photocatalytic activity of polycrystalline ZnO/TiO_2 systems. 2. Surface, bulk characterization, and 4-nitrophenol photodegradation in liquid-solid regime. *J. Phys. Chem. B* **2001**, *105* (5), 1033−1040.

(19) Evgenidou, E.; Konstantinou, I.; Fytianos, K.; Poulios, I.; Albanis, T. Photocatalytic oxidation of methyl parathion over TiO_2 and ZnO suspensions. *Catal. Today* **2007**, *124* (3−4), 156−162.

(20) Zhonghai, Z.; Yuan, Y.; Yanju, F.; Linhong, L.; Hongchun, D.; Litong, J. Preparation of photocatalytic nano-ZnO/TiO_2 film and application for determination of chemical oxygen demand. *Talanta* **2007**, *73* (3), 523−528.

(21) Peternel, I. T.; Koprivanac, N.; Loncaric-Bozic, A. M.; Kusic, H. M. Comparative study of UV/TiO_2, UV/ZnO and photo-Fenton processes for the organic reactive dye degradation in aqueous solution. *J. Hazard. Mater.* **2007**, *148* (1−2), 477−484.

(22) Wang, C.; Xu, B. Q.; Wang, X. M.; Zhao, J. C. Preparation and photocatalytic activity of ZnO/TiO_2/SnO_2 mixture. *J. Solid State Chem.* **2005**, *178* (11), 3500−3506.

(23) Khan, A. Y.; Mazyck, D. W. The effect of UV irradiation on adsorption by activated carbon/TiO_2 composites. *Carbon* **2006**, *44* (1), 182−184.

(24) So, C. M.; Cheng, M. Y.; Yu, J. C.; Wong, P. K. Degradation of azo dye Procion Red MX-5B by photocatalytic oxidation. *Chemosphere* **2002**, *46* (6), 905−912.

(25) Hu, C.; Tang, Y. H.; Jiang, Z.; Hao, Z. P.; Tang, H. X.; Wong, P. K. Characterization and photocatalytic activity of noble-metal-supported surface TiO_2/SiO_2. *Appl. Catal., A* **2003**, *253* (2), 389−396.

(26) Hasnat, M. A.; Siddiquey, I. A.; Nuruddin, A. Comparative photocatalytic studies of degradation of a cationic and an anionic dye. *Dyes Pigm.* **2005**, *66* (3), 185−188.

(27) Hurum, D. C.; Agrios, A. G.; Gray, K. A.; Rajh, T. Thurnauer, M. C. Explaining the enhanced photocatalytic activity of Degussa P25 mixed-phase TiO_2 using EPR. *J. Phys. Chem. B* **2003**, *107* (19), 4545−4549.

(28) Lin, H.; Huang, C. P.; Li, W.; Ni, C.; Shah, S. I.; Tseng, Y. H. Size dependency of nanocrystalline TiO_2 on its optical property and photocatalytic reactivity exemplified by 2-chlorophenol. *Appl. Catal., B* **2006**, *68* (1−2), 1−11.

(29) Teoh, W. Y.; Amal, R.; Madler, L.; Pratsinis, S. E. Flame sprayed visible light-active Fe-TiO_2 for photomineralisation of oxalic acid. *Catal. Today* **2007**, *120* (2), 203−213.

Received for review September 17, 2007
Revised manuscript received November 21, 2007
Accepted November 30, 2007

IE071255P